

The Ring Formation Mechanism in Cyclization of Berberine

Guosheng Wang*, Siyu Han and Ronghui Xu

Shenyang University of Chemical Technology, Liaoning Shenyang, 110142 Yuelan Wang, Xinjiang University, Xinjiang Wulumuqi, 830046.

wgsh-lyc@163.com*

(Received on 3rd July 2019, accepted in revised form 2nd December 2020)

Summary: Berberine hydrochloride is a natural alkaloid with significant antitumor activities against many types of cancer cells, can be synthesized by cyclic reaction with hydrochloride condensate and glyoxal as raw materials and copper chloride as catalyst. In this study, the transition and energy change for the each reaction step was calculated by the density functional theory program Dmol³ in Materials Studio 2017. and the results testified that there are two ring formation in the cyclization process, and according to the result we proposed the mechanism of this cyclization reaction. We also use infrared and ultraviolet spectroscopy to monitor the reaction process in real time and prove the ring formation process. The reaction mechanism was firstly proposed at the basic results of above.

Keywords: Berberine, Cyclic reaction, DFT, Reaction mechanism.

Introduction

The copper-based catalyst has been widely used as an efficient oxidant in the cyclization reaction, especially, in coupling reactions through C-N or C-O bond coupling [1-8]. In the copper base catalysts, both CuCl₂/copper(α)-chloride [9-16] and CuCl/cuprous-chloride [17-24] used as single electron oxidant in the cyclization reaction have been attracted more and more attention, as a result of the features such as inexpensive, readily available, high region-selectivity, easy operation, and good yields. Many research groups proposed the mechanism of the cyclization reaction catalyzed by CuCl₂ or CuCl based on the experimental results and the computation study by the density functional theory (DFT). The catalytic cycle of Cu(α/β) replaced by CuCl₂ or CuCl used respectively has been accepted generally [25-29]. The catalytic cyclization process is likely to be initiated by the nucleophilic addition, radical addition or electrophilic addition to produce a copper divalent complex or firstly reducing Cu divalent complex to Cu monovalent complex by condensation with an electron transfer, Subsequently oxidative addition of the Cu monovalent complex to form a Cu trivalent complex, the oxidation either by air or by Cu itself, finally the Cu trivalent complex is reduced, to regenerated the Cu divalent or Cu monovalent catalysts.

The study on the catalytic action of copper chloride and cuprous chloride in the same cyclization reaction is rare [30, 31], the results indicate that the copper chloride is beneficial to the intramolecular, compared with the reaction of cuprous chloride in the intramolecular catalysis, and the copper chloride has a higher coordination capability and rate determining

free energy barrier than cuprous chloride in the same cyclization reaction. So far, the combined or synergistic effects of CuCl₂ and CuCl in the cyclization reaction have not been reported.

Berberine hydrochloride is an agent with effective antibacterial, antituber, anti-inflammatory and anti-HIV et. Properties [32-35]. There are also lots of reports on anticancer properties of Berberine hydrochloride against a variety of different cells. Due to the ability to form strong complexes with nucleic acids, the anticancer activity of berberine hydrochloride appears [36, 37]. The research on the cocrystal of Berberine hydrochloride and other anticancer compounds synergistic anticancer effect and the anticancer nanomaterials supported by berberine hydrochloride are hot topics nowadays [38-40]. Berberine hydrochloride has been synthesized for more than 40 years, and the CuCl₂-catalyzed cyclization reaction mechanism has not been established. On the basis of the experimental results and relevant reports in the literature, we firstly proposed the reaction mechanism of CuCl₂-catalyzed cyclization of N-(2',3'-dimethoxy benzyl)-3,4-dioxy-methylene-phenylethylamine hydrochloride and glyoxal, and investigated by density functional theory (DFT) to understand the activity of CuCl₂/CuCl in the cyclization reaction.

Experimental and Computational Methods

Chemicals

Hydrochloride condensates(98%,Northeast Pharmaceutical Group Limited,China), Glacial acetic acid(99.5 % , Tianjin Damao Chemical Factory,

*To whom all correspondence should be addressed.

China), Acetic anhydride(99.5 % , Tianjin Yongda Chemical Reagent Co., Ltd, China), Glyoxal(99%, Tianjin Yongda Chemical Reagent Co., Ltd, China), Copper chloride (99 % , Tianjin Yongda Chemical Reagent Co., Ltd, China), Copper chloride(99 % , Tianjin Yongda Chemical Reagent Co., Ltd, China), Hydrochloric acid (36%, Tianjin Yongda Chemical Reagent Co., Ltd, China), Hydrogen peroxide($\geq 30\%$, Tianjin Yongda Chemical Reagent Co., Ltd, China). All solutions were prepared using 18.2 M Ω deionized water (Millipore).

Real-time analysis

The study started with the reaction of copper(α) chloride, glyoxal, and N-(2',3'-dimethoxy benzyl)-3,4-dioxy-methylene-phenylethylamine hydrochloride in acetic acid at 117°C for 2 hours. Then the intermediate was oxidized by the hydrogen peroxide under the presence of HCl at 30°C for 30 mins. Finally, refined the product. And the yield was 81%. The decrement control of water content in the system was achieved by adding acetic anhydride (Scheme-1) and real-time monitoring analysis by infrared and ultraviolet analysis was conducted in the cyclization reaction.

DFT Calculation

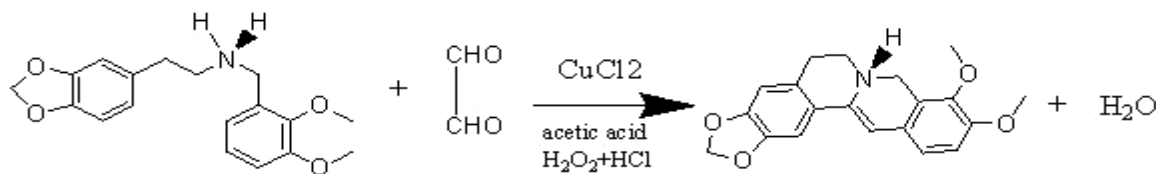
The simulation can be performed by the density functional theory program Dmol 3 in Materials Studio 2017 [36, 37]. During the simulation, spin unrestricted geometry optimization and single-point energy calculations are performed, the DNP double numerical basis set is used. The core electrons are treated with DFT semi-core pseudo-potentials (DSPP). The exchange-correlation energy was calculated using the Perdew-Burke-Ernzerhof (PBE) generalized gradient approximation (GGA). A Fermi smearing of 0.005 Ha and a global orbital cutoff of 4.0 Å are employed. The convergence criteria for the geometric optimization and energy calculation are set as follows: (a) a self-consistent field tolerance of 1.0×10^{-5} Ha/atom, (b) an energy tolerance of 2.0×10^{-5} Ha/atom, (c) a maximum force tolerance of 0.004 Ha /Å, and (d) a maximum displacement tolerance of 0.005 Å. The density mixing is used to accelerate the convergence, to explore the transfer of electric charge and the strength of the bond, the population is calculated. The transition state (TS) is determined by using of the linear and quadratic synchronous transi

(LST/QST) complete search method. And the frequency is calculated to ensure the credibility of TS at the same time, and to consider the weak interaction, the TS method for DFT-D is used in the simulation process.

Results and Discussion

Real-time IR spectra

The reaction process was monitored in real time, and the samples collected in the process were tested by infrared and ultraviolet spectroscopy. The infrared spectrogram is shown in Fig. 1. As can be seen from the IR spectra monitored in Fig. 1, the four peaks with different intensities, located at 1600 cm⁻¹, 1580 cm⁻¹, 1500 cm⁻¹ and 1450 cm⁻¹, belong to the C=C skeleton vibration characteristic peak on the benzene ring, while 880-680cm⁻¹ belong to the out-of-plane vibration of C-H, and C-H stretching vibration on the typical benzene ring located at 3100-3000 cm⁻¹. It belongs to Ar-O stretching vibration at 1270-1230cm⁻¹ and C-O stretching vibration located at 1050-1000cm⁻¹. The peaks locate at 3500-3100cm⁻¹ belong to N-H vibration, and 1420-1400cm⁻¹ belong to C-N vibration. As the reaction time went on, the N-H stretching peaks which are at the position of 3400cm⁻¹ changed from the constant obvious peak of N-H in the raw material to the non-obvious one, and then gradually disappeared, it shows that N-H bond condensed with copper chloride. The first ring formed at 80min after reaction, and then go on. the stretching vibration of the aldehyde groups (C=O) characteristic peaks are at 1750-1700cm⁻¹ gradually appeared, and reached the maximum at 80 minutes, this indicates that two aldehyde group of glyoxal condensed with copper chloride firstly, and then one aldehyde group of glyoxal at the other end of the intermediate was exposed with the first hydroxylation of a carbonyl group. The peak value at 1750-1700cm⁻¹ disappears after the time of 120 minutes; it can prove that the reaction process is carried out in sequence. In other words, C-N bonded with one aldehyde group of glyoxal, complexde with copper chloride, and then oxidized with Ar-H on the benzene ring to form the first six-membered ring. Finally, the aldehyde group on the other end of glyoxal, under the synergistic action of copper chloride and cuprous chloride, oxidized with Ar-H on the benzene ring to form the second six-membered ring.



Scheme-1: The Cyclic Reaction of Berberine Hydrochloride.

Real-time UV spectra

Fig 2 shows the real-time monitoring of UV-vis Spectroscopic of the reaction. As can be seen, the UV-vis Spectroscopic of hydrochloride condensation compound displays at 275nm, which is characteristic absorption peaks of aromatic compounds. As the reaction time, goes on, the absorption peak displays at 500nm and 700nm gradually appear. According to this change trend, it proves that transition from aromatic ring to condensed ring in turn and the benzene ring structure formed in the process of reaction. This is consistent with the inference.

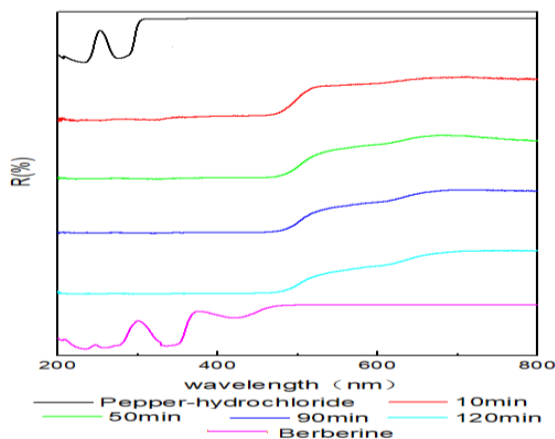


Fig. 2: Real-time UV-vis Spectroscopic.

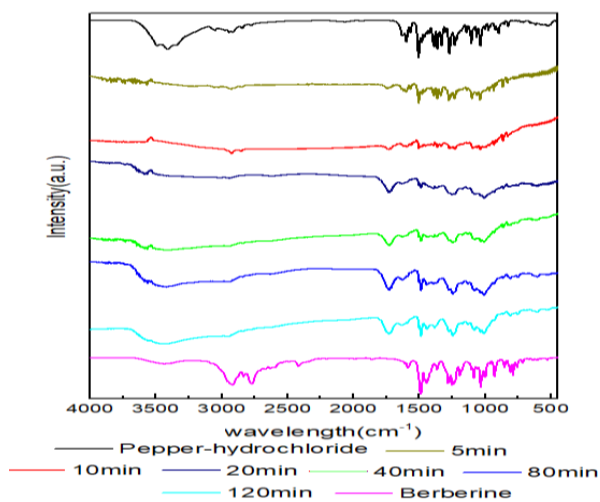


Fig. 1: Real-time IR spectra.

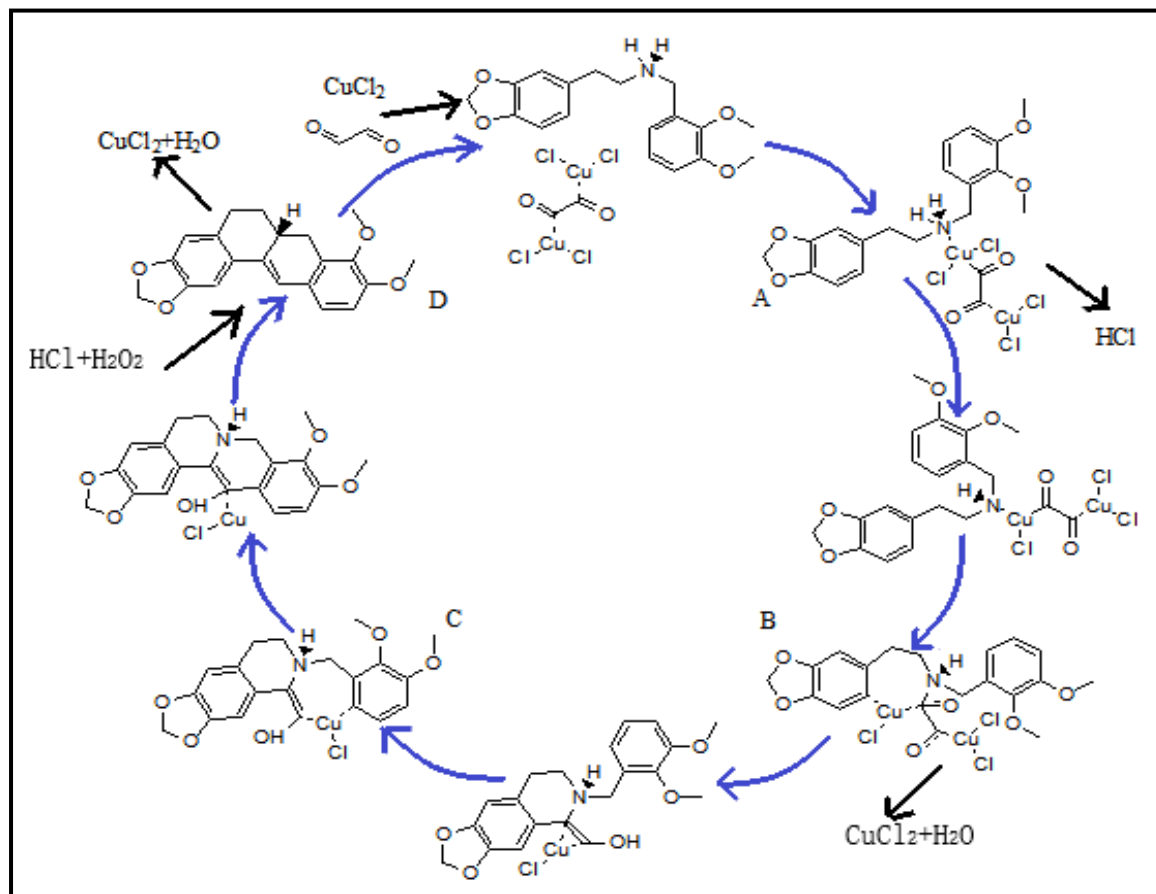
Reaction Steps

A set of the transition state, energy barrier, and energy change for each reaction step calculated were shown in Table-1, it can be seen that the first six-membered ring intermediate formed via a transition state (TS5) with an activation energy of $E_a=175.60\text{kJ/mol}$, the calculated result indicates that this process is the rate determining step with the first six-membered ring formation and the second six-membered ring intermediated formed via a transition state(TS7) with an activation energy of $E_a=146.66\text{kJ/mol}$. The calculation shows that there are two steps to form the successive rings in the cyclic reaction process.

Table-1: Transition state, required activation energy and free energy barrier of each step.

	Reactions	Transitions state	E_a (kJ/mol)	ΔH (kJ/mol)
R1	CC and GIC complexation			-1.25
R2	Drop HCl			-1.45
R3	N and C connection	TS1	12.54	-69.47
R4	First cyclization	TS2	20.26	1.35
R5	Produce first OH	TS3	42.45	31.84
R6	Produce second OH	TS4	57.89	-65.61
R7	Break Cu-C			5.21
R8	Drop first H ₂ O	TS5	175.60	21.23
R9	Second cyclization	TS6	68.50	-117.71
R10	Break Cu-C	TS7	146.66	33.77
R11	Drop second H ₂ O(with CuCl ₂)	TS8	57.89	-152.45

Mechanism



Scheme-2: Proposed Mechanism of the Cu-Catalyzed Reaction.

On the basis of the experimental and calculated results and literature precedents, a proposed mechanism for the cyclization reaction was shown in Scheme-2. The Cu(α/β) catalytic cycle would proceed through the intermediate A, generated from a coordination of copper(α)-chloride and aldehyde and imino group in the reactants, subsequent a seven-membered ring intermediate B formed by proton transfer and dehydrogenation of intermediate A, and in this process HCl was dropped. The second seven-membered ring intermediate C formed through dehydration by synergistic catalytic action of Cu(α) /Cu(I) with the first six-membered ring B formation. As a result of Cu-C broke and hydroxy generated, CuCl₂ and H₂O were dropped in this process. Finally, final product D provided by oxidation and elimination of Cu(I) complexes underwent the presence of HCl and hydrogen peroxide (broke Cu-C), and the copper catalyst regenerated. The catalytic cycle and the transition state of the reaction process were shown with the removal and addition of HCl, H₂O and CuCl₂ were

generated from the deprotonation and oxidation reaction, and the second dehydration and CuCl₂ regeneration assisted the hydrogen peroxide under the presence of HCl.

Conclusion

Discontinuous sampling analysis method was used to real-time analysis by infrared and ultraviolet analysis, the changes of the stretching vibration of N-H and the aldehyde group (C=O) indicate that the cyclization process was gradually formed as reaction time goes on. The DFT calculated results testify that there are two ring formations in the cyclization process, the first six-membered ring intermediate formed via a transition state with an activation energy of $E_a=175.60\text{kJ/mol}$ and the second six-membered ring intermediated formed via a transition state with an activation energy of $E_a=146.66\text{kJ/mol}$. The cyclization mechanism which includes two cyclic steps is first proposed.

Acknowledgements

This work was supported by the National Natural Science Foundation of China (No. 51402199, 51422210), and Liaoning province science and technology project.(2017230001)

References

1. Y. F. Chen, J. C. Hsieh, Synthesis of polysubstituted phenanthridines via ligand-free copper-catalyzed annulation, *Org. Lett.*, **16**, 4642 (2014).
2. V. Kavala, C. C. Wang, D. K. Barange, C. W. Kuo, P. M. Lei, C. F. Yao, Synthesis of isocoumarin derivatives via the copper-catalyzed tandem sequential cyclization of 2-halo-N-phenyl benzamides and acyclic 1,3-diketones, *J. Org. Chem.*, **77**, 5022 (2012).
3. S. Manna, A. P. Antonchick, Copper(I)-catalyzed radical addition of acetophenones to alkynes in furan synthesis, *Org. Lett.*, **17**, 4300 (2015).
4. C. Gronnier, S. Kramer, Y. Odabachian, F. Gagosz, Cu(I)-catalyzed oxidative cyclization of alkynyl oxiranes and oxetanes, *J. Am. Chem. Soc.*, **134**, 828 (2012).
5. Á. Sinai, D. Vangel, T.Gáti, P. Bombicz, Z. Novák, Utilization of copper-catalyzed carboarylation–ring closure for the synthesis of new oxazoline derivatives, *Org. Lett.*, **17**, 4136 (2015).
6. C. W. Cheung, S. L. Buchwald, Room temperature copper(II)-catalyzed oxidative cyclization of enamides to 2,5-disubstituted oxazoles via vinylic C–H functionalization, *J. Org. Chem.*, **77**, 7526 (2012).
7. X. Y. Zhu, M. Li, Y. P. Han, S. Chen, X. S. Li, Y. M. Liang, Copper-catalyzed oxidative cyclization of alkynes with sulfonylhydrazides leading to 2-sulfonated 9H-pyrrolo[1,2-a]indol-9-ones, *J. Org. Chem.*, **82**, 8761 (2017).
8. C. Wan, J. Zhang, S. Wang, J. Fan, Z. Wang, Facile Synthesis of polysubstituted oxazoles via a copper-catalyzed tandem oxidative cyclization, *Org. Lett.*, **12**, 2338 (2010).
9. M. Nishino, K. Hirano, T. Satoh, M. Miura, Copper-catalyzed oxidative direct cyclization of N-methylanilines with electron-deficient alkenes using molecular oxygen, *J. Org. Chem.*, **76**, 6447 (2011).
10. M. Jithunsa, M. Ueda, O. Miyata, Copper(II) chloride-mediated cyclization reaction of N-alkoxy-ortho-alkynylbenzamides, *Org. Lett.*, **13**, 518 (2011).
11. Y. Y. Jhang, T. T. Fan-Chiang, J. M. Huang, J. C. Hsieh, Copper-catalyzed annulation: A method for the systematic synthesis of phenanthridinium bromide, *Org. Lett.*, **18**, 1154 (2016).
12. J. Sun, F. Wang, H. Hu, X. Wang, H. Wu, Y. Liu, Copper(II)-catalyzed carbon–carbon triple bond cleavage of internal alkynes for the synthesis of annulated indolizines, *J. Org. Chem.*, **79**, 3992 (2014).
13. Y. Liu, J.W. Sun, Copper(II)-catalyzed synthesis of benzo[f]pyrido[1,2-a]indole-6,11-dione derivatives via naphthoquinone difunctionalization reaction, *J. Org. Chem.*, **77**, 1191 (2012).
14. C. Y. Huang, V. Kavala, C. W. Kuo, A. Konala, T. H. Yang, C. F. Yao, Synthesis of biologically active indenoisoquinoline derivatives via a one-pot copper(II)-catalyzed tandem reaction, *J. Org. Chem.*, **82**, 1961 (2017).
15. Z. Chen, J. Chen, M. Liu, J. Ding, W. Gao, X. Huang, H. Wu, Unexpected copper-catalyzed cascade synthesis of quinazoline derivatives, *J. Org. Chem.*, **78**, 11342 (2013).
16. J. N. Zhu, L. L. Chen, R. X. Zhou, B. Li, Z. Y. Shao, S. Y. Zhao, Copper-catalyzed oxidative cyclization of maleimides with amines and alkyne esters: Direct access to fully substituted dihydropyrroles and pyrrole derivatives, *Org. Lett.*, **19**, 6044 (2017).
17. X. Zeng, L. Ilies, E. Nakamura, Synthesis of functionalized 1H-indenes via copper-catalyzed arylative cyclization of arylalkynes with aromatic sulfonyl chlorides, *J. Am. Chem. Soc.*, **133**, 17638 (2011).
18. Q. Wu, Y. Zhang, S. Cui, Divergent Syntheses of 2-aminonicotinonitriles and pyrazolines by copper-catalyzed cyclization of oxime ester, *Org. Lett.*, **16**, 1350 (2014).
19. D. Yang, Y. L. Yan, B. F. Zheng, Q. Gao, N. Y. Zhu, Copper(I)-catalyzed chlorine atom transfer radical cyclization reactions of unsaturated α -chloro β -keto esters, *Org. Lett.*, **8**, 5757 (2006).
20. Á. Sinai, Á. Mészáros, T. Gáti, V. Kudar, A. Palló, Z. Novák, Copper-catalyzed oxidative ring closure and carboarylation of 2-ethynylanilides, *Org. Lett.*, **15**, 5654 (2013).
21. A. Prieto, D. Bouyssi, N. Monteiro, Copper-catalyzed double C–H alkylation of aldehyde-derived N,N-dialkylhydrazones with polyhalomethanes: Flexible access to 4-functionalized pyrazoles, *ACS Catal.*, **6**, 7197 (2016).
22. Y. Huang, X. Li, Y. Yu, C. Zhu, W. Wu, H. Jiang, Copper-mediated oxidative cyclization reaction

- of N-tosylhydrazones and β -ketoesters: Synthesis of 2,3,5-trisubstituted furans, *J. Org. Chem.*, **81**, 5014 (2016).
23. X. F. Xia, L. L. Zhang, X. R. Song, X. Y. Liu, Y. M. Liang, Copper-catalyzed oxidative cyclization of enynes for the synthesis of 4-carbonyl-quinolines with O₂, *Org. Lett.*, **14**, 2480 (2012).
24. B. Yuan, R. He, W. Shen, C. Huang, M. Li, Mechanistic insights into the Cu(I)- and Cu(II)-catalyzed cyclization of o-alkynylbenzaldehydes: The solvent DMF and oxidation state of copper affect the reaction mechanism, *J. Org. Chem.*, **80**, 6553 (2015).
25. J. Aziz, G. Frison, M. Gómez, J. D. Brion, A. Hamze, M. Alami, Copper-catalyzed coupling of N-tosylhydrazones with amines: Synthesis of fluorene derivatives, *ACS Catal.*, **4**, 4498 (2014).
26. K. Kubota, E. Yamamoto, H. Ito, Copper(I)-catalyzed borylative exo-cyclization of alkenyl halides containing unactivated double bond, *J. Am. Chem. Soc.*, **135**, 2635 (2013).
27. Y. Zhao, J. Qiu, L. Tian, Z. Li, M. Fan, J. Wang, New copper(I)/DBU catalyst system for the carboxylative cyclization of propargylic amines with atmospheric CO₂: An experimental and theoretical study, *ACS Sustainable Chem. Eng.*, **4**, 5553 (2016).
28. M. A. Celik, M. Yurtsever, N. Ş. Tüzün, F. Ş. Güngör, Ö. Sezer, O. Anaç, Metal-catalyzed cyclization reactions of carbonyl ylides: Synthesis and DFT study of mechanisms, *Organometallics*, **26**, 2978 (2007).
29. E. S. Sherman, P. H. Fuller, D. Kasi, S. R. Chemler, Pyrrolidine and piperidine formation via copper(II) carboxylate-promoted intramolecular carboamination of unactivated olefins: diastereoselectivity and mechanism, *J. Org. Chem.*, **72**, 3896 (2007).
30. N. Kundu, A. Roy, D. Banik, N. Sarkar, Unveiling the mode of interaction of berberine alkaloid in different supramolecular confined environments: Interplay of surface charge between nano-confined charged layer and DNA, *J. Phys. Chem. B.*, **120**, 1106 (2016).
31. C. Wang, S. R. Perumalla, R. Lu, J. Fang, C. C. Sun, Sweet berberine, *Cryst. Growth Des.*, **16**, 933 (2016).
32. J. Liu, X. LUO, R. GUO, W. Jing, H. LU. cell Metabolomics Reveals Berberine-Inhibited Pancreatic Cancer Cell Viability and Metastasis by Regulating Citrate Metabolism [J]. *J. Proteome. Res.*, **19**, 3825 (2020).
33. F. Papi, C. Bazzicalupi, M. Ferraroni, G. Ciolli., P. Lombardi, A. Y. Khan, G. S. Kumar, P. Gratteri, Pyridine Derivative of the Natural Alkaloid Berberine as Human Telomeric G4DNA Binder: A Solution and Solid-State Study[J].*ACS.Med.Chem.Lett.*,**11**,645-650(2020).
34. Q. Han, H. Tang, M. Zou, J. Zhao, L. Wang Z, Bian, Y. Li. Anti-inflammatory Efficacy of Combined Natural Alkaloid Berberine and S1PR Modulator Fingolimod at Low Doses in Ulcerative Colitis Preclinical Models [J]. *J. Nat. Prod.*, **83**, 1939 (2020).
35. E. Laudadio, N. Cedraro, G. Mangiaterra, B. Citterio ,G. Mobbili,C. Minnelli, D. Bizzaro, F. Biavasco, R. Galeazzi. Natural Alkaloid Berberine Activity against Pseudomonas aeruginosa MexXY-Mediated Aminoglycoside Resistance: In Silico and in Vitro Studies [J]. *J. Nat. Prod.*, **82**, 1935 (2019).
36. H. -P. Kuo, T. -C. Chuang, M. -H. Yeh, S. -C. Hsu, T. -D. Way, P. -Y. Chen, S. -S. Wang, Y. -H. Chang, M. -C. Kao, J. -Y. Liu. Growth Suppression of HER2-Overexpressing Breast Cancer Cells by Berberine via Modulation of the HER2/PI3K/Akt Signaling Pathway[J]. *J.Agt. Food. Chem.*, **59**, 8216 (2011).
37. R. Bhanumathi, M. Manivannan, R. Thangaraj, S. Kannan. Drug-Carrying Capacity and Anticancer Effect of the Folic Acid- and Berberine-Loaded Silver Nanomaterial To Regulate the AKT-ERK Pathway in Breast Cancer[J]. *ACS Omega*, **3**, 8317 (2018).
38. H. -P. Kuo, T. -C. Chuang, S. -C. Tsai, H. -H. Tseng, S. -C. Hsu, Y. -C. Chen, C. -L. Kuo, Y. -H. Kuo, J. -Y. Liu, M. -C. Kao. Berberine, an Isoquinoline Alkaloid, Inhibits the Metastatic Potential of Breast Cancer Cells via Akt Pathway Modulation[J]. *J.Agt. Food. Chem.*, **60**, 9649 (2012).
39. H. -P. Kuo, T. -C. Chuang, S. -C. Tsai, H. -H. Tseng, S. -C. Hsu, Y. -C. Chen, C. -L. Kuo, Y. -H. Kuo, J. -Y. Liu, M. C. Kao. Growth Suppression of HER2-Overexpressing Breast Cancer Cells by Berberine via Modulation of the HER2/PI3K/Akt Signaling Pathway[J]. *J.Agt. Food. Chem.*, **59**, 8216 (2011).